Influence of Grain Size on the Structure, Electrical Properties and the Phase Transition Temperature of Nano $La_{0.72}Sr_{0.28}mno_3$ Perovskite Employing in – Situ Ultrasonic Measurement

M. Vigneswari
Department of Physics
PSR College of Engineering, Sevalpatti – 626 140
Sivakasi, Tamil Nadu, India
Research Scholar in Physics, Manonmaniam Sundaranar University
Tirunelveli, Tamil Nadu, India

K. Sakthipandi[1], S. Sankarrajan[2]
Department of Physics
[1]Sethu Institute of Technology, Kariapatti - 626 115, Tamil Nadu, India
[2]Unnamalai Institute of Technology, Kovilpatti - 628 503
Tamil Nadu, India

***Abstract*—The solid state reaction method followed by the ball milling technique was used to synthesize the nano sized $La_{0.72}Sr_{0.28}MnO_3$ (LSMO) perovskite samples with different grain size of 43, 35, 30, 23, 16 nm. The rhombohedral structures present in the prepared perovskites were explored through the X – ray diffraction (XRD) measurements. The functional groups present in nano sized LSMO perovskites were obtained through the recorded Fourier Transform Infrared spectroscopy (FTIR) pattern. The microscopic studies revealed that the particle sizes of the nano LSMO perovskite samples were 10 – 130 nm. The temperature dependence of the measured electrical properties indicates the semiconductor nature of nano LSMO perovskite sample. The ultrasonic velocities and attenuation were further measured at a frequency of 20 MHz over a wide range of temperatures from 300 to 400 K. The occurrence of ferro-paramagnetic transition temperature (T_c) was explored through the observed anomalous behavior in ultrasonic velocities, attenuations and elastic moduli. Moreover, the observation made from the XRD pattern of nano LSMO perovskite samples were in line with the peak broadening in the ultrasonic studies at the phase transition. The particle size dependent critical constants for the density, ultrasonic velocities and attenuations (both longitudinal and shear) were also obtained**

Keywords*— *Perovskites; nano particle; Ultrasonic measurements; Elastic properties; Phase Transition

I. INTRODUCTION

The development of new materials for technological applications in various electronic devices like sensors, switches, actuators etc., has been intensively studied in the present century [1, 2]. The nano sized perovskite manganite materials with a chemical composition of $R_{1-x}A_xMnO_3$, (where R-trivalent rare earth elements and A- divalent alkaline earth ions) which has been one of the true engineering materials exhibiting novel physical properties [3]. These materials have been widely used for the growth of new materials for different potential applications such as spanning energy production in solid oxide fuel cell [4], radioactive waste encapsulation for environmental containment, dielectric resonator materials for communication systems and magnetic sensors [5,6]. $La_{1-x}Sr_xMnO_3$ (LSMO) perovskite material has been the most attractive material due to its high Curie temperature (T_c) and colossal magnetoresistance (CMR) arises because of strong mutual coupling of spin, charge and lattice degrees of freedom [7].

In recent years, $La_{1-x}Sr_xMnO_3$ mixed valent perovskite materials with doping concentration of "x" varying between 0.1 and 0.4 are vital due to their interesting physico- chemical properties [8]. $LaMnO_3$ with doping of strontium ($x > 0.2$) exhibit high amount of ionic conductivity, chemical stability and high spin polarization of the charge carrier. Hence, it has been acting as cathode in solid oxide fuel cell over a wide range of temperatures (600 – 900 K) [9]. Arao et al [10] have reported the occurrence of the structural phase transition in lightly doped LSMO ($0 < x < 0.08$) simple perovskite oxides. These lightly doped perovskites are electron insulators. The phase transition from ferromagnetic (FM) followed by antiferromagnetic (AFM) phase at higher temperatures for the concentration of $0.1 < x < 0.15$ have been reported [11]. The perovskites with $0.17 < x < 0.6$ is metallic with a ferromagnetic ground state caused by the double exchange (DE) mechanism between the Mn^{3+} and Mn^{4+} ions [12].

Literature survey has revealed that a lot of studies have been carried out on nanoscale maganites due to their novel magnetic properties like CMR, giant magnetoresistance (GMR), optical properties, thermal and electronic properties [13,1,2]. The nano structured perovskite materials have been widely used for many areas such as storage devices, nano medicine, molecular computing nano photonics tunable resonant devices, catalysts, sensors, magnetic refrigeration and spin valve devices. Moreover, the properties of manganite in nanoscale particles have been easily understood by comparing with the results of the different grain sizes of the manganite materials [14]. The grain size reduction has played a vital role to determine the rich variety of electronic phases [15]. The

performance of the nano structured materials has been increased with a transition temperature [16]. The mangnetically disordered state of the grains has increased due to the reduction in particle size. Grain size dependent $La_{0.67}Sr_{0.33}MnO_3$ has been shown that the material exhibiting the large magnetic moment and high value of FM – paramagnetic (PM) transition temperature (370 K). It has been reported that the reduction of grain size has led to increase of resistivity [17]. It is interesting to note that the structural disorder happening near the grain boundary that leads to the DE mechanism causing of intrinsic CMR effect, that result in spin disorder and suppression of phase transition [16].

Various methods have been used to prepare the nano sized LSMO perovskite manganites at different particle size such as ball milling method [18], sonochemical method [19], electrochemical deposition [20], magnetron sputtering [21], pulse laser deposition [22], sol-gel [23], hydrothermal [24], spray pyrolysis [25]. The ball milling method is a simplest process compared to other techniques, which has received much attention as a powerful tool for the synthesis of several advanced functional materials [26]. Generally, the transition temperature (T_c) of nano LSMO perovskite materials have been depend on density, grain size, porosity and atomic diffusibility [27]. Thus, the correlation of particle size with T_c has been very important tool to understand the structural and magnetic properties of nano LSMO perovskite materials.

In the present investigation, the structural, vibrational and electrical properties of the nano sized $La_{0.72}Sr_{0.28}MnO_3$ (LSMO) perovskites were characterized by X – ray diffraction measurement, Fourier Transform Infrared spectroscopy, Brunauer – Emmeet – Teller (BET) surface area measurement, High resolution scanning electron microscope (HRSEM), Transmission electron microscope (TEM) and conductivity studies. In-situ ultrasonic velocities and attenuation measurements were also made over a wide range of temperature using an indigenously designed experimental set-up. The particle size dependent transition temperature of the prepared nano LSMO perovskite samples has revealed from observed anomalies in the ultrasonic parameters.

II. EXPERIMENTAL DETAILS

A. *Preparation of sample*

The nano structured $La_{0.72}Sr_{0.28}MnO_3$ perovskite samples of various grain sizes were prepared from high purity lanthanum nitrate (99.99%, Alfa Alsar), strontium nitrate (99.99%, Alfa Alsar), manganese carbonate (99.99%, Alfa Alsar) and citric acid (99.99%, Alfa Alsar) by conventional solid state reaction technique followed by the ball milling technique (Fritsch Planetary Monomill, Germany). The stoichiometric ratio of the base materials were measured and grounded. The mixture was calcined twice at 723 K for 2 h in air (Lenton Wire Chamber Furnace, Germany). Further, the calcined powders were subjected to high energy ball milling with intermediate grounding. Small amount of milled powder was taken out from the bowl after 30 mins, 60 mins, 90 mins, 120 mins and 150 mins milling to check the formation of nanostructured material and the samples were denoted as LSMO1, LSMO2, LSMO3, LSMO4 and LSMO5 respectively. Finally, samples were pressed into pellets with a diameter of 13 mm and then, sintered at 1273 K for 12 h in atmospheric air. The sintered pellets were used for further characterization.

For structural study, X – ray diffraction measurements were conducted using BRUKER AXS D8 advanced XRD, (USA). The density of nano sized LSMO samples were measured employing Archimedes principle using the CCl4 liquid as buoyant. For vibrational studies, FTIR measurement was made with SHIMADZU – IR Affinity – 1 Spectrometer, USA in the wave number range of 4000 – 400 $^{cm-1}$. BET surface area analyser (Autosorb – 1,Quantachrome, USA) was used to determine the surface area of the prepared nano sized LSMO perovskite samples [28]. To study the morphology of the prepared samples, HRSEM, (Quanta FEG 250, Netherlands) was used to carried out. The images obtained by using a TEM (CM 200; Philips, USA) were used to reveal the sub structural information and particle size of the samples. Electrical conductivity was obtained using HIOKI 3351 – 01 LCR Hi tester (France) in the range between 50 Hz to 1 MHz at various temperatures [29]. Further, the ultrasonic velocities and attenuation (both longitudinal and shear) were measured by using through transmission method over the wide range of temperatures from 300 to 400 K at the heating rate of 0.5 K min^{-1} [30].

III. RESULTS & DISCUSSION

The XRD patterns of nano sized LSMO powder ball milled at various time have shown in Fig. 1.

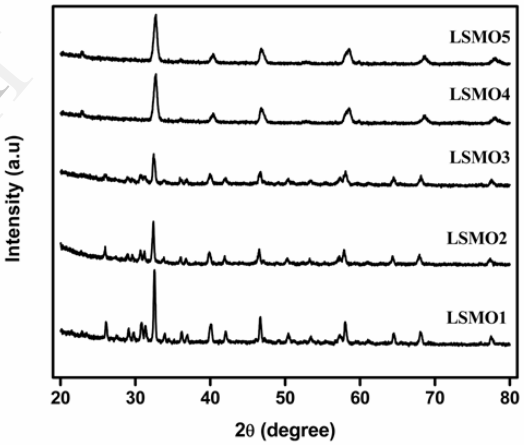

Fig. 1. Experimental X-ray patterns of $La_{0.72}Sr_{0.28}MnO_3$ sample ball milled at 30,60,90,120 and 150 mins respectively for LSMO1, LSMO2, LSMO3, LSMO4 and LSMO5

The observed XRD pattern have confirmed the crystalline nature of the prepared samples. It is curious to note that all the peaks of the prepared sample has emerged out as an uniform crystalline phase with the maximum intensity planes at [104] for LSMO1,LSMO2,LSMO3 and [110] planes for LSMO4, LSMO5 respectively. The prepared nano LSMO perovskite samples have rhombohedral structure with R3C space group [JCPDS file no: 89 – 8098] [17]. The crystalline size of nano LSMO perovskite samples have been obtained by using Scherrer's formula. They have been 43, 35, 30, 23 and 16 nm for LSMO1, LSMO2, LSMO3, LSMO4 and LSMO5 respectively. The obtained grain size denotes the grain size of the nano LSMO perovskite which decreases with the increase in milling time. A shift in diffraction angle (2θ) to a lower value and broader peaks in smaller grain size nano LSMO perovskite samples when compared with larger grain size nano LSMO perovskite samples were observed. The nano LSMO5

perovskite sample has large full width half maximum value (0.5292) when compared with nano LSMO1 perovskite sample (0.1989). The standard peaks of XRD has broadened out from nano LSMO1 perovskite sample to nano LSMO5 perovskite sample which in turn revealed that the width of the diffraction peak increased with decreasing grain size, since the grain size is reduced, the DE interaction has been weakening due to the mobility of conduction electrons in the nano LSMO perovskite samples [31].

The density of nano sized LSMO perovskite with different grain size was measured. The values of the densities are 6515, 6389, 6154, 5842 and 5714 kg/m^3 for LSMO1, LSMO2, LSMO3, LSMO4 and LSMO5 respectively. The grain size dependent density is shown in Fig. 2.

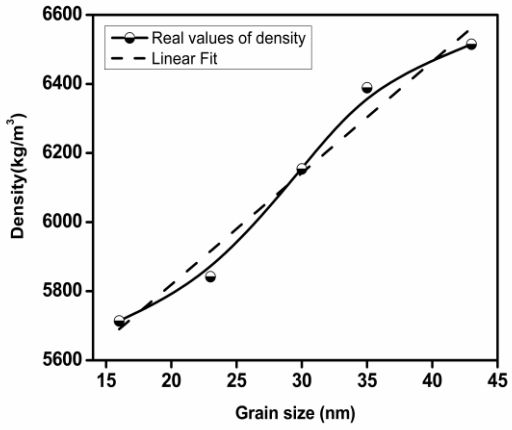

Fig 2 Grain size dependent density of nano $La_{0.72}Sr_{0.28}MnO_3$ sample ball milled at 30,60,90,120 and 150 mins

The density of the nano sized LSMO perovskite manganite material is significantly decreased with the decrease in grain size. It is interesting to observed that the reduction of grain size from 43 to 16 nm has led to decrease in the density from 6515 to 5714 kg/m^3. The physical parameters like density of the samples have played a vital role in determining the structural, electrical and magnetic properties [32].

The FTIR spectrum of nano sized LSMO1 perovskite sample is shown in Fig. 3.

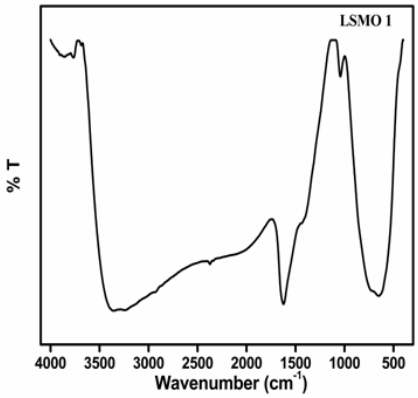

Fig 3 FTIR spectra of the nano $La_{0.72}Sr_{0.28}MnO_3$ sample ball milled at 30 mins (LSMO1)

The band observed at 600 cm^{-1} has been IR active that correspond to the combination of stretching mode of Mn-O-Mn and bending mode of Mn-O bonds. The peak observed at 1623 cm^{-1} corresponds to deformation mode of water molecule [33]. The peaks in the higher wave number ranging 3300 – 3900 cm^{-1}, reveals the stretching vibration of the O – H molecule.

The HRSEM image of nano LSMO perovskite samples has been shown in Fig. 4.

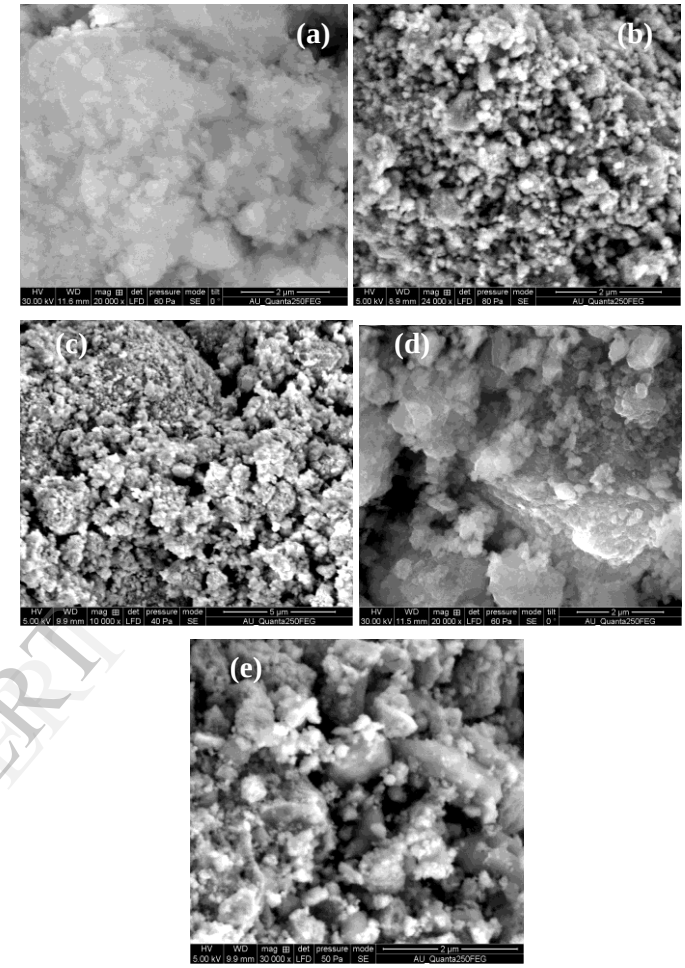

Fig. 4 (a – e). HRSEM micrograph of nano $La_{0.72}Sr_{0.28}MnO_3$ sample ball milled at 30,60,90,120 and 150 mins

All the images have been inherently uniform and have shown an agglomerated spherical like morphology with undistributed pores. The particle sizes estimated from HRSEM images and the values are 126, 117, 116, 99, 90 nm for LSMO1, LSMO2, LSMO3, LSMO4 and LSMO5 respectively. The decrease in surface area during synthesis leads to a decrease in particle size is observed in the synthesized nano LSMO perovskite samples [34]. It is also clear that from HRSEM microcraphs the particles are highly agglomerated with irregular boundaries due to the high homogenousity during synthesis at various milling time [35].

The TEM image of nano LSMO perovskite samples has been shown in Fig. 5. It is clear that the prepared nano LSMO perovskite samples are dissimilar and distributed in different sizes. The approximate particle size estimated from TEM images. The particle sizes are 41, 33, 27, 21 and 15 nm respectively for LSMO1, LSMO2, LSMO3, LSMO4 and LSMO5 respectively. Further it is clear from the TEM images that the particle size decreases with increase in milling time.

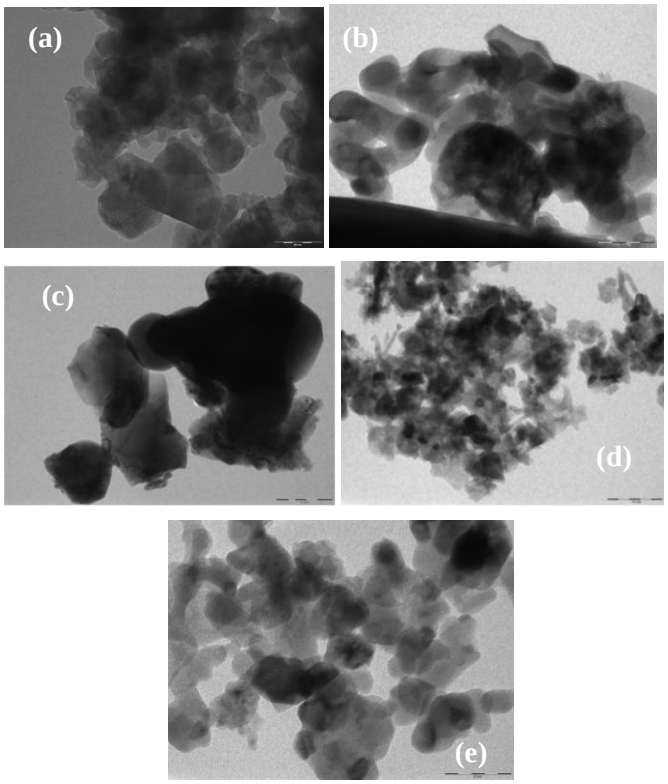

Fig. 5 (a –e). TEM micrograph of nano $La_{0.72}Sr_{0.28}MnO_3$ sample ball milled at at 30,60,90,120 and 150 mins

The BET surface area of the synthesized nano LSMO perovskite samples have been measured [28]. The measured BET surface area for the synthesized nano LSMO1, LSMO2, LSMO3, LSMO4 and LSMO5 perovskite samples are 23, 29, 35, 48 and 72 m^2g^{-1} respectively. It has inferred that the surface area increases with a decrease in grain size. The equivalent spherical diameter (DBET) have been determined by measuring the surface area and the density of perovskite samples and the values are 40, 32, 28, 21 and 15 nm for LSMO1, LSMO2, LSMO3, LSMO4 and LSMO5 respectively. The D_{BET} of the samples decrease with an increase in milling time. This is in close agreement with the grain size from XRD results [36].

The a.c impedance technique has been a powerful tool for characterizing the electrical properties of materials. Fig. 6a shows the typical impedance real (Z′) and imaginary (Z″) impedance values of nano LSMO1 perovskite sample during temperature range of 300 to 400 K. The ionic conductivity of the sample was found. The bulk conductivity has been calculated from the impedance plot and has been found to be 1.29×10^{-8}, 4.26×10^{-8}, 6.10×10^{-8} and 9.18×10^{-7} S cm^{-1} at 300, 360, 370 and 400 K for nano LSMO1 perovskite sample respectively. It has been observed that the conductivity increases with the increase in temperature. This indicates that the prepared nano LSMO perovskite sample have been in semiconductor nature [37].

The conductivity of the nano LSMO1 is investigated at different temperatures over a wide range of frequencies. The frequency dependent conductivity spectrum of nano LSMO1 perovskite sample is shown in Fig. 6b which has shown a low frequency dc plateau and a high frequency dispersive region. The dc conductivity value has been determined. The conductivity values of nano LSMO1 perovskite sample at different temperatures are shown in Table 1.

Table 1: Temperature dependence conductivity of nano sized LSMO1 perovskite sample

Temperature (K)	Conductivity (S cm^{-1})
300	1.29×10^{-8}
360	4.26×10^{-8}
370	6.10×10^{-8}
400	9.18×10^{-7}

In the region of 370 K, there is a dramatic changes in conductivity behavior has occurred. This has been attribute possible phase transition and Jahn- Teller distortion (JT), which is prominent in LaMnO3 based materials [38]. This may perhaps extensively vary the orbital overlapping and subsequently the hopping of electrons along with the adjacent Mn ions.

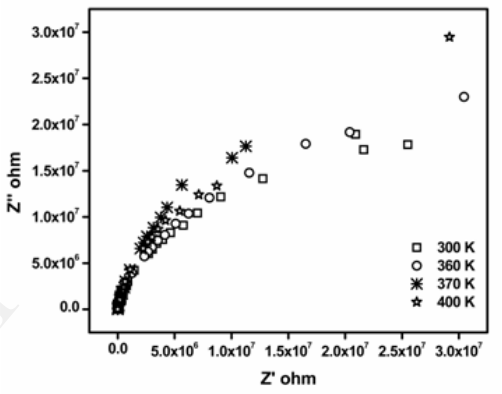

Fig. 6a. Complex impedance plot of nano $La_{0.72}Sr_{0.28}MnO_3$ sample ball milled at 30 mins (LSMO1) at various temperatures

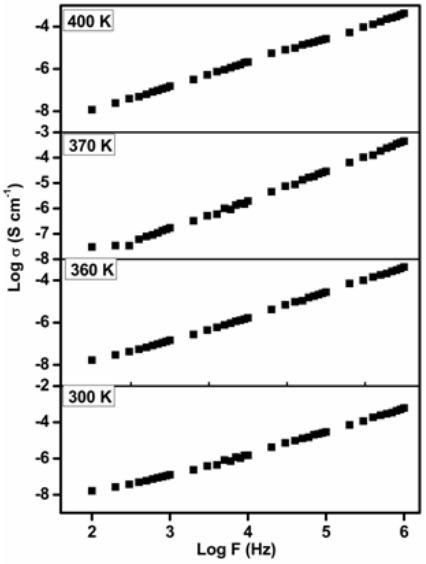

Fig. 6b. The frequency dependent conductivity spectrum of nano $La_{0.72}Sr_{0.28}MnO_3$ sample ball milled at 30 mins (LSMO1) at various temperatures

The longitudinal, shear ultrasonic velocities and attenuation measurements of nano LSMO perovskite samples were carried out at room temperature. Fig. 7a – 7d displays the grain size dependent of ultrasonic parameters of nano LSMO perovskites.

A linear increase in longitudinal ultrasonic velocity (U_L) is observed with a decrease in grain size. Consequently for attenuation (α_L), it decreases with a decrease in grain size. A similar trend has been observed in shear velocity (U_S) and its attenuation (α_S) of U_L and α_L respectively of nano sized LSMO perovskite samples. An increase in ultrasonic velocity and a decrease in attenuation has been obtained with the decrease in grain size. The disordered surface layers and less stored defect is observed in the nano LSMO perovskite materials by reduction of grain size during the synthesis [39].

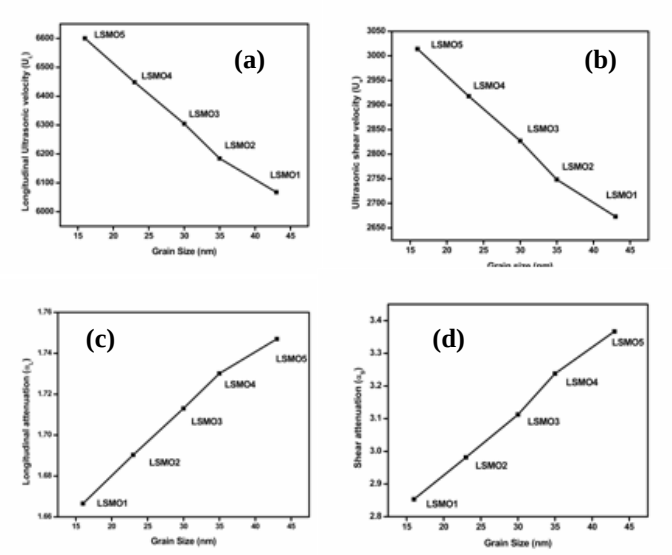

Fig. 7 (a –d). Ultrasonic parameters with various grain size of nano $La_{0.72}Sr_{0.28}MnO_3$ perovskite sample at room temperature

As temperature increases, a linear decrease in velocities and an increase in attenuation have been observed in the absence of structural/phase transitions for any magnetic materials [40]. The existence of phase / structural transition in perovskite samples leads to dip/peak in velocity/ attenuation [41]. In the present study, the velocities and attenuation as a function of temperature of nano LSMO perovskite materials from 300 to 400 K are measured and are shown in Figs. 8 and 9.

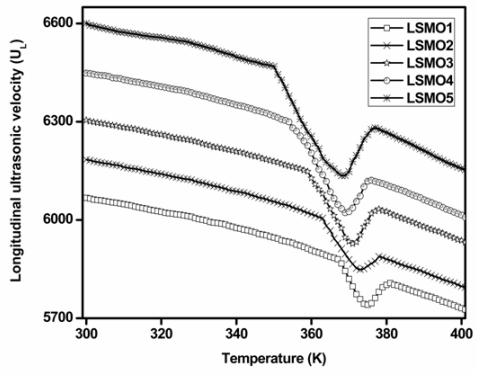

Fig. 8. Temperature dependence of Longitudinal ultrasonic velocity of nano $La_{0.72}Sr_{0.28}MnO_3$ sample ball milled at 30,60,90,120 and 150 mins (LSMO1, LSMO2, LSMO3, LSMO4 and LSMO5 respectively)

It is interesting to observe that there is an anomalous behaviour of U_L and U_S instead of an expected linear variation has been obtained as a function of temperature. For nano LSMO1 perovskite sample, a monotonic decrease in velocity is noted from 300 to 367 K and 381 to 400 K.

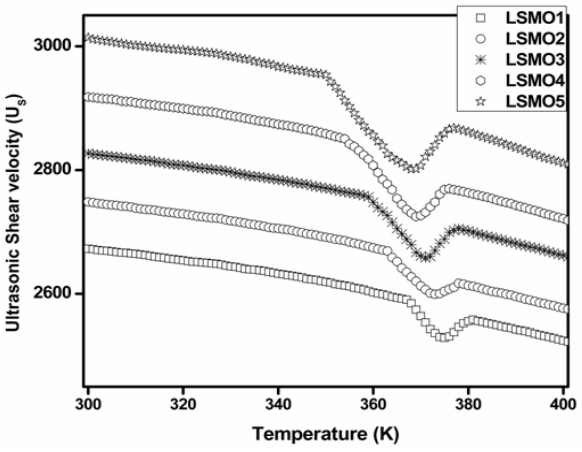

Fig. 9. Temperature dependence of Shear ultrasonic velocity of nano $La_{0.72}Sr_{0.28}MnO_3$ sample ball milled at 30,60,90,120 and 150 mins (LSMO1, LSMO2, LSMO3, LSMO4 and LSMO5 respectively)

An anomalous behaviour is noted in the temperature ranging from 367 to 381 K and it is used to study the structural/phase transitions in nano LSMO perovskite samples. It is clear seen that at the temperature of 367 K there is a sharp dip in velocity starts and reaches a minimum at 375 K and further an increase in temperature beyond 375 K leads to sharp rise in velocity up to 381 K. Similarly, the dip in velocities for LSMO2, LSMO3, LSMO4 and LSMO5 are observed for 373, 371, 369 and 368 K respectively. A similar behaviour in U_S is observed as that of U_L. α_L and α_S as a function of temperature has shown a reverse trend to the velocities as shown in Figs. 10 and 11.

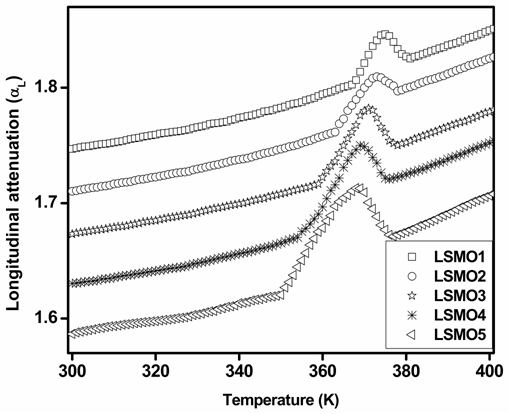

Fig. 10. Temperature dependence of Longitudinal ultrasonic attenuation of nano $La_{0.72}Sr_{0.28}MnO_3$ sample ball milled at 30,60,90,120 and 150 mins (LSMO1, LSMO2, LSMO3, LSMO4 and LSMO5 respectively)

The observed dip in velocities and peak in attenuations of nano LSMO perovskite samples have been correlated with magnetic transition temperature, using the phase diagram of both bulk and nano LSMO perovskite samples [42, 36]. It is inferred that the temperature at which the minima in velocities is related the FM – PM transition temperature of nano LSMO perovskite samples. Thus the temperature 375, 373, 371, 369 and 368 K are denoted as T_c of LSMO1, LSMO2, LSMO3, LSMO4 and LSMO5 respectively. It is clear that the T_c value decreases with a decrease in particle size. As the particle size is

reduced, the short range magnetic interaction between Mn^{3+} and Mn^{4+} ions is distorted due to the large number of grain boundaries. It has been responsible for the suppression of T_c and reduction in magnetization [43].

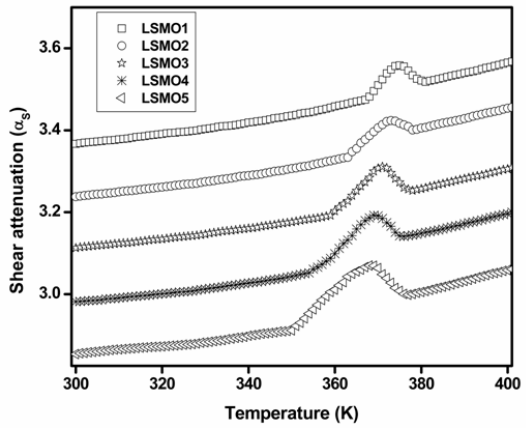

Fig. 11. Temperature dependence of Ultrasonic shear attenuation of nano $La_{0.72}Sr_{0.28}MnO_3$ sample ball milled at 30,60,90,120 and 150 mins (LSMO1, LSMO2, LSMO3, LSMO4 and LSMO5 respectively)

Fig.12 displays the particle size dependent T_C of synthesized nano LSMO perovskite samples. It is evident from the Fig.12, it is clearly seen that, when the particle size is reduced from LSMO1 to LSMO5 nano perovskite samples, the T_C value decreases from 375 to 368 K. Further one can easily identify the unknown size of the particles from the plot of particle size dependent T_C.

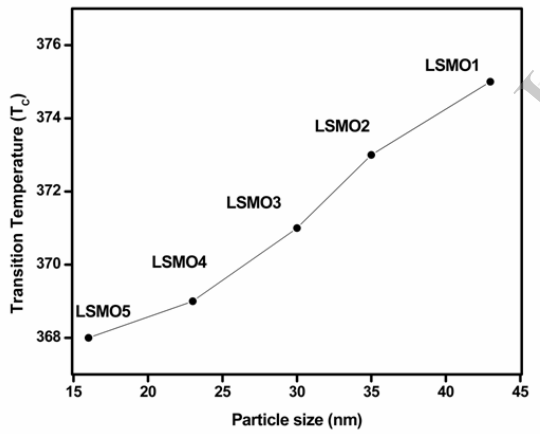

Fig. 12. Particle size dependent Transition temperature (T_C) of nano $La_{0.72}Sr_{0.28}MnO_3$ sample ball milled at 30,60,90,120 and 150 mins

The lattice softening and lattice hardening of the perovskite manganite materials have been correlated with an increase and a decrease in velocity respectively [41]. The occurrence of peak height is directly correlated to lattice softening at the transition temperature [43]. Hence from the Fig. 8 and 9 it is seen that the lattice hardening and lattice softening are gradually increased from LSMO1 to LSMO5 nano perovskite sample. It is due to the existence of strong electron – phonon coupling, when the particle size is reduced. Moreover, the observation made from the XRD pattern for nano sized LSMO perovskite samples is in line with peak broadening in ultrasonic studies at phase transition [33].

Further the transition width (ΔT_c) of the nano LSMO perovskite samples has been noted and as listed in Table. 2.

Table 2: Temperature range of anomalous region of nano sized LSMO perovskite sample

Anomalous Temperature	LSMO1	LSMO2	LSMO3	LSMO4	LSMO5
Start (K)	367	363	359	354	350
End (K)	381	379	378	376	375
Anomaly (K)	375	373	371	369	368

It is observed that the transition width is wider when the particle size is reduced. It indicates that the diffused ferromagnetic phase transition is observed with a decrease of particle size. Hence, from the observed anomaly in ultrasonic velocities and attenuations one can clearly understand an abrupt change in coupling between spin, charge, orbital and lattice degrees of freedom and interactions at transition temperature of nano sized LSMO perovskite samples [44]. The observed results show direct evidence for spin–phonon couplings of nano sized LSMO perovskite samples. Thus, in – situ ultrasonic measurements have been useful in exploring the structural and phase transition behaviour in nano sized LSMO perovskite manganite materials. Further it is interesting to note that as the particle size is decreasing, the T_c is also decreasing.

IV. CONCLUSION

In-situ ultrasonic velocity and attenuation studies on nano sized LSMO perovskite samples reveal that T_c decreases with the decrease in particle size. The lattice hardening and lattice softening increases when the particle size is reduced. It is due to the existence of strong electron – phonon coupling when the particle size is reduced. Moreover, the observation made from the XRD pattern for nano sized LSMO perovskite samples is in line with the peak broadening in ultrasonic studies at phase transition. The transition width is wider when the particle size is reduced. It indicates that the diffused ferromagnetic phase transition is observed with a decrease in particle size. In addition, the wider transition width observed at T_c reveals weakening the double exchange (DE) interactions.

REFERENCES

[1] V. Dyakonov, A. S´ lawska-Waniewska, N. Nedelko, E. Zubov, V. Mikhaylov, K. Piotrowski, A. SzytuŁa, S. Baran, W. Bazela, Z. Kravchenko, P. Aleshkevich, A.Pashchenko, K. Dyakonov, V. Varyukhin, H. Szymczak, "Magnetic, resonance and transport properties of nano powder of $La_{0.7}Sr_{0.3}MnO_3$ manganites", J. Magn. Magn. Mater, vol. 322, pp. 3072–3079, June 2010.

[2] P. Van Cuong, D. H. Kim, "Effect of strontium doping level on electrical transport and magnetic properties of $La_{1-x}Sr_xMnO_3$ perovskite nanoparticles", J. Phys. Conf. Ser, vol. 187, pp. 012090, 2009.

[3] G. Van Tendeloo, O. I. Lebedev, S. Amelinckx, "Atomic and microstructure of CMR Materials", J. Magn. Magn. Mater. vol. 211, pp. 73 – 83, 2000.

[4] S. P. Jiang and J. G. Love, "Origin of the initial polarization behavior of Sr-doped LaMnO3 for O2 reduction in solid oxide fuel cells", Solid State Ionics, vol. 138, pp. 183-190, 2001.

[5] M. M. Sutar, A. N. Tarale, S. R. Jigajeni, S. B. Kulkarni, P. B. Joshi, "Investigations on nanocrystalline BST-LSMO magnetodielectric composites", Appl Nanosci, vol.2, pp. 311-317, September 2012.

[6] W. J. Lu, X. Luo, C. Y. Hao, W. H. Song, Y. P. Sun, "Magnetocaloric effect and Griffiths-like phase in $La_{0.67}Sr_{0.33}MnO_3$ nanoparticles", J. Appl. Phys, vol. 104, pp. 113908-1 – 113908-6, October 2008.

[7] S. Y. Yang, W. L. Kuang, C. H. Ho, W. S. Tse, M. T. Lin, S. F. Lee, Y. Liou, Y. D. Yao, "Magnetoresistance of $La_{0.7}Sr_{0.3}MnO_3$ film at room temperature", J. Magn. Magn. Mater. vol. 226–230, pp. 690 – 692, 2001.

[8] S. M. Haile, "Fuel cell materials and components", Acta Mater, vol. 51, pp. 5981– 6000, August 2003.

[9] A. J. Campbell, G. Balakrishnan, M. R. Lees, D. McK. Paul, "Single-crystal neutron- diffraction study of a structural phase transition induced by a magnetic field in La_{1-x} Sr_x MnO_3, Phys. Rev, vol. B 55, PP. 8622–8625, 1977.

[10] M. Arao, T. Veno, T. Asada, Y. Koyama, C. Minamisawa, M. Mogi, Y. Inoue, Physica C. Superconductivity, (2004) 171 –177

[11] F. Paraskevopoulos, C. Mayr, A. Hartinger, J.pimenov, Hemberger, P. Lunkenheimer, A. Loidl, A. Mukhin, V. Yu. Ivanov, A. M. Balbashov, "The phase diagram and optical properties of $La_{1-x}Sr_xMnO_3$ for x<0.2", J. Magn. Magn. Mater, vol.211, pp. 118 – 127, 2000.

[12] H. Y. Hwang, S. W. Cheong, N. P. Ong, "Spin-Polarized Intergrain Tunneling in $La_{2y3}Sr_{1y3}MnO_3$", Phys. Rev. Lett, vol.77, pp. 2041 – 2044,September 1996.

[13] M. Mori, M. N. Sammes, E. Suda, Y. Takeda, "Application of $La_{0.6}AE_{0.4}MnO_3$ (AE=Ca and Sr) to electric current collectors in high-temperature solid oxide fuel cells", Solid State Ionics, vol. 0167 – 2738, pp. 1 – 15, 2003.

[14] S. Roy, I. Dubenko, D. D. Edorh, N. Ali, "Size induced variations in structural and magnetic properties of double exchange $La_{0.8}Sr_{0.2}MnO_{3-\delta}$ nano-ferromagnet", J.Appl.Phys, vol. 96, pp. 1202 – 1208, April 2004.

[15] E. Dagotto, "Nanoscale phase separation and colossal magnetoresistance", Springer series in solid state ionics, vol. 136, pp. 453, 2003.

[16] P. Kameli, H. Salamati, A. Aezami, "Influence of grain size on magnetic and transport properties of polycrystalline $La_{0.8}Sr_{0.2}MnO_3$ manganites", Journal of Alloys and Compounds, vol. 4500925 – 8388, pp. 1–11, 2008.

[17] R. PanneerMuthuselvam, N. Bhowmik, "Grain size dependent magnetization, electrical resistivity and magnetoresistance in mechanically milled $La_{0.67}Sr_{0.33}MnO_3$",Journal of Alloys and Compounds, vol.511. pp.22 – 30, 2012.

[18] I. Panagiotopoulos, N. Moutis, M. Ziese, A. Bollero, "Magnetoconductance and hysteresis in milled $La_{0.67}Sr_{0.33}MnO_3$ powder compacts", J. Magn. Magn. Mater. vol. 299, pp. 94 – 104, 2006.

[19] P. Van Cuong, J. Dho, H. Yeol Park, D. Hyung Kim, 'A sonochemical-assisted synthesis and annealing temperature effect of $La_{0.7}Sr_{0.3}MnO_3$ nanoparticles", J. App. Physics A, vol.95, pp. 567 – 571, 2009.

[20] G.S. Pang, Xu, X.N.; V. Markovich, S. Avivi, O. Palchik, Y. Koltypin, G. Gorodetsky, Y. Yeshurun, H.P. Buchkremer, and A. Gedanken "Preparation of $La_{(1-X)}sr_xmn_{o(3)}$ Nanoparticles by Sonication-Assisted Coprecipitation" Mater. Res. Bull., vol. 38, , pp. 11-16, (2003).

[21] Z. Yang, L. Sun, C. Ke, X. Chen, W. Zhu, O. Tan, "Growth and structure properties of $La_{1-x}Sr_xMnO_{3-\sigma}$ (x=0.2, 0.3, 0.45) thin film grown on SrTiO3 (0 0 1) single-crystal substrate by laser molecular beam epitaxy", J. Cryst. Growth. Vol 311, pp3289-3294, (2009)

[22] T. R. McGuire, A. Gupta, R. P. Duncombe, M. Rupp, J.Z. Sun, R. B. Laibowitz, W. J. Gallager, X. Gang, "Magnetoresistance and magnetic properties of $La_{\{1-x\}}sqrt(n)_{\{x\}}MnO_{\{3-delta\}}$ thin films", J. Appl. Phys. Vol.79, pp 4549- 4551, (1996)

[23] Rostamnejadi,H.Salamati,P.Kameli, H. Ahmadvand,"Superparamagnetic behavior of $La_{0.67}Sr_{0.33}MnO_3$ nanoparticles prepared via sol–gelmethod", J. Magn. Magn. Matter, vol. 321, pp. 3123 – 3131, 2009.

[24] T.Y. Chen, K. Z. Fung, "Synthesis of and densification of oxygen-conducting $La_{0.8}Sr_{0.2}Ga_{0.8}Mg_{0.2}O_{2.8}$ nano powder prepared from a low temperature hydrothermal urea precipitation process", J. Eur. Ceram. Soc, vol. 28, pp. 803 – 810, 2008.

[25] A. Abrutis, A. Teiserskis, G. Garcia, V. Kubilius, Z. Saltyte, Z. Salciunas, V. Faucheux, A. Figueras, S. Rushworth, "Preparation of dense, ultra-thin MIEC ceramic membranes by atmospheric spray-pyrolysis technique", J. Membr. Sci, vol. 240, pp. 113 – 122, 2004.

[26] K. Zhang, T. Holloway, J. Pradhan, M. Bahoura, R Bah, R. R. Rakhimov, A. K . Pradhan, R. Prabakaran, "Synthesis and magnetic characterizations of $La_{(1-x)}Sr_{(x)}MnO_3$ nanoparticles for biomedical applications." J. Nanosci Nanotechnol. vol 10, pp.5520 – 5526, 2010.

[27] S. Das, P. Chowdhury, T. K Gundu Rao, D. Das, D. Bahadur, "Influence of grain size and grain boundaries on the properties of $La_{0.7}Sr_{0.3}Co_xMn_{1-x}O_3$", Solid State Commun, vol. 1210038 – 1098, pp. 691 – 695, 2002.

[28] M. Rezaei, M. Khajenoori, B. Nematollahi, "Preparation of nanocrystalline MgO by surfactant assisted precipitation method", Mater. Res. Bull, vol. 46, pp. 1632– 1637, 2011.

[29] N. Rajeswari, S. Selvasekarapandian, S. Karthikeyan, M. Prabu, G. Hirankumar, H. Nithya, C. Sanjeeviraja, "Conductivity and dielectric properties of polyvinyl alcohol–polyvinylpyrrolidone poly blend film using non-aqueous medium", J.Non Crystalline Solids, vol. 357, pp. 3751–3756, 2011.

[30] V. Rajendran, N. Palanivelu, P. Palanichamy, T. Jayakumar, Baldev Raj, B.K.Chaudhuric, "Ultrasonic characterisation of ferroelectric $BaTiO_3$ doped lead bismuth oxide semiconducting glasses", vol. 296, pp. 39 – 49, December 2001.

[31] S. Daengsakul, C. Thomas, I. Thomas, C. Mongkolkachit, S. Siri, V. Amornkitbamrung, S. Maensiri, "A simple thermal decomposition synthesis, magnetic properties and cytotoxicity of $La_{0.7}Sr_{0.3}MnO_3$ nanoparticles", Appl Phys A, vol. 96, pp. 691 – 699, 2009.

[32] T. D. Shen, J. Zhang, Y. Zhao, "What is the theoretical density of a nanocrystalline material" Acta Mater. Vol 56, 3663–3671, (2008).

[33] M. Quijada, J. Cerne, J. R. Simpson, H. D. Drew,K. H.Ahn, A. J. Millis, R. Shreekala, R. Ramesh, M. Rajeswari, T. Venkatesan, "Optical conductivity of manganites: Crossover from Jahn-Teller small polaron to coherent transport in the ferromagnetic state", Phys. Rev. B, vol. 58, pp. 16093 – 102, 1998.

[34] A. Gedanken, "Using sonochemistry for the fabrication of nanomaterials", vol. 11, pp. 47 – 55, April 2004.

[35] Z.F. Zi, Y.P. Sun, X.B. Zhu, Z.R. Yang, J.M. Dai, W.H. Song, "Synthesis of magnetoresistive $La_{0.7}Sr_{0.3}MnO_3$ nanoparticles by an improved chemical coprecipitation method", J. Magn. Magn, Matter, vol. 321, pp. 2378 – 2381, 2009.

[36] P. Kulandaivelu , K.Sakthipandi , P.SenthilKumar , V.Rajendran, "Mechanical properties of bulk and nanostructured $La_{0.61}Sr_{0.39}MnO_3$ perovskite manganite materials Journal of Physics and Chemistry of Solid, vol. 74, pp. 205 – 214, 2013.

[37] R.J. Wiglusz, A. Gaki, G. Kakali, A. Chuchma, W. Strek, "Conductivity and electric properties of $La_{1-x}Sr_xMnO_{3-\delta}$ nanopowders", Journal of rare earths, Vol 27, pp651- 654, (2009).

[38] G. Lehmann, P. Hess, S. Weissmantel, G. Reisse, P. Scheible, A. Lunk, "Young's modulus and density of nanocrystalline cubic boron nitride films determined by dispersion of surface acoustic waves", Appl. Phys. A, vol. 74, pp. 41 – 45,2002.

[39] L. Godfrey, J. Philip, "Ultrasonic measurement of the elastic constants of LiKSO4 between 300 and 370 K", Solid State Commun, vol. 97, pp. 635 – 638, 1996.

[40] R. K. Zheng, C. F. Zhu, J. Q. Xie, R. X. Huang, X.G. Li, "Charge transport and ultrasonic properties in $La_{0.57}Ca_{0.43}MnO_3$ perovskite", Mater. Chem. Phys, vol. 75, pp. 121 – 124, 2002.

[41] Q. J. Huang, Y. Cheng, X. J. Liu, X. D. Xu, S. Y. Zhang, "Study of the elastic constants in a $La_{0.6}Sr_{0.4}MnO_3$ film by means of laser-generated ultrasonic wave method", Ultrasonics, vol. 44, pp. 1223 – 1227, 2006.

[42] L. Hueso, N. D. Mathur, "Nanotechnology: Dreams of a hollow future", Nature, vol. 427, pp. 301 – 304, 2004.

[43] R. K. Zheng, C .F. Zhu, and X. G. Li, "Magnetic Field Dependent on Ultrasonic Sound Velocity and Attenuation in Charge-Ordering Manganese Oxide $La_{0.5}Ca_{0.5}MnO_3$" Phys. Status Vol 184 (2001) 251–256.

[44] S. Singh, S. B. Krupanidhi, "Synthesis and structural characterization of $Ba_{0.6}Sr_{0.4}TiO_3$ nanotubes , Phys. Lett. A, vol. 367, pp. 356 – 359, 2007.